

# Determination of activation effect of $\text{Ca}(\text{OH})_2$ upon the hydration of BFS and related heat by isothermal calorimeter

L'ubomír Ježo · Martin Palou · Jana Kozánková · Tomáš Ifka

CCTA10 Special Issue  
© Akadémiai Kiadó, Budapest, Hungary 2010

**Abstract** Isothermal conduction calorimetry, differential thermal analysis (DTA)–thermogravimetric analysis (TG) analysis, and SEM observations have proved the activation effect of  $\text{Ca}(\text{OH})_2$  released from the  $\text{C}_3\text{S}$  hydration upon blast furnace slag (BFS). Five sample mixtures of BFS and  $\text{C}_3\text{S}$  and two samples of pure BFS and  $\text{C}_3\text{S}$  were submitted to reaction with water inside the calorimeter at room temperature. The values of hydration heat were recorded up to 7 days. Samples were stored in humidity during 28 days and then were submitted to DTA–TG and SEM analysis. The effect of  $\text{Ca}(\text{OH})_2$  upon heat evolution of sample mixtures has been quantified and its influence upon the formation of new hydrates and microstructure of pastes was evidenced.

**Keywords** Puzzolanic activation · Thermal analysis · Heat evolution · Microstructure

## Introduction

Cement is an inorganic powder material consisting of minerals  $3\text{CaO}\cdot\text{SiO}_2$  ( $\text{C}_3\text{S}$ ),  $2\text{CaO}\cdot\text{SiO}_2$  ( $\text{C}_2\text{S}$ ),  $3\text{CaO}\cdot\text{Al}_2\text{O}_3$  ( $\text{C}_3\text{A}$ ), and  $4\text{CaO}\cdot\text{Al}_2\text{O}_3\cdot\text{Fe}_2\text{O}_3$  ( $\text{C}_4\text{AF}$ ) formed by solid-state reaction among  $\text{CaO}$ ,  $\text{SiO}_2$ ,  $\text{Al}_2\text{O}_3$ , and  $\text{Fe}_2\text{O}_3$  present

Cement chemistry nomenclature and abbreviations used through this article: C =  $\text{CaO}$ , S =  $\text{SiO}_2$ , A =  $\text{Al}_2\text{O}_3$ , F =  $\text{Fe}_2\text{O}_3$ , CC =  $\text{CaCO}_3$ , H =  $\text{H}_2\text{O}$ , CH =  $\text{Ca}(\text{OH})_2$ .

L. Ježo  
PCLA, Cement Plant, Ul. Jána Kráľ'a 1, Ladce, Slovak Republic

M. Palou (✉) · J. Kozánková · T. Ifka  
Division of Ceramics, Glass and Cement, Faculty of Chemical and Food Technology, Bratislava, Slovak Republic  
e-mail: martin.palou@stuba.sk

in a finely ground and homogenized raw mixture [1]. After burning, clinker is milled with gypsum or other calcium sulfate compound as set regulator to give ordinary Portland cement (OPC). The production of OPC clinker, which is carried out at 1450 °C, needs energy and lime-bearing raw material; therefore, the huge quantity of limestone and fuel is consumed releasing thus  $\text{CO}_2$ . Emission of  $\text{CO}_2$  becomes a pertinent matter that producers of cements must deal with. The addition to cement of suitable industrial wastes or by-products such as ground blast-furnace slag, fly ashes, silica fume forms blended cements [2–5]. The production and use of blended cements are considered as alternative to OPC for many reasons including environment protection (depletion of  $\text{CO}_2$ , large-scale use of industrial wastes, and by-products), energy saving (reduction of clinker part in cement), and technical requirements (low hydration heat, durability of concrete, sulfate resistance, etc.).

The use of cements in civil and engineering construction as binder materials is linked to their reaction with water, so-called hydration. Indeed, hydration of pure Portland cement is a multi-stage and heterogeneous chemical reaction of individual clinker minerals with water in the presence of gypsum to form stable hydrated products causing setting and hardening of cement pastes or concrete. This complex process involves dissolution of primary minerals, nucleation, crystal growth, and microstructure evolution that ensures chemical, physical, and mechanical properties of concretes or cement pastes. The hydration of cement and the accompanying phenomena are described as exothermic processes and the heat generated can be determined by means of calorimetry [6–13]. Therefore, different types of commercial [11] and self-developed laboratory [12] calorimeters have been used to record the exothermic reaction of cement with water considering temperatures (adiabatic or semi-adiabatic and isoperibolic calorimeters) or heat

flow (isothermal or heat-conduction calorimeters) as outputs.

The relationship between these methods has not been established yet, even though their calorimetric behavior (dependence of temperature or heat evolution on time) presents the same features characterized by the same stages.

The use of calorimetry in cement chemistry is an indispensable way to determine, not only the hydration heat, but also to investigate the influences of factors such as temperatures, admixtures, fineness, water cement ratio, mineralogical composition upon the kinetics (acceleration or retardation process) of cement hydration [13–15]. Based on calorimetric measurements, Kada-Benameur et al. [14] have proposed a mathematical model describing hydration degree as function of temperatures and hence (apparent) activation energy of hydration of cements was determined [13–16]. Blended cements containing blast furnace slag (BFS) are the most worldwide used because of the abundance of slag. Ground BFS is a by-product resulting from iron-making process and rapidly quenched in air. Slag alone is hydraulically latent. The activation of slag by any way leads to the formation of binder materials such as cement paste. Therefore, many studies [2, 15–17] were undertaken in order to understand the principle and mechanism of the activation of slag. Indeed,  $\text{Ca}(\text{OH})_2$ , water glass, and alkalis can react with slag components to form main hydration products such as CSH and CASH by pozzolanic reaction [18]. In blended cements,  $\text{Ca}(\text{OH})_2$  is released from hydration of  $\text{C}_3\text{S}$  and  $\text{C}_2\text{S}$  at initial period which then reacts with BFS. The hydration heat of blended cements due to the effect of  $\text{Ca}(\text{OH})_2$  released from  $\text{C}_3\text{S}$  and  $\text{C}_2\text{S}$  is not yet fully established. Many studies [2, 3, 15, 18, 19] have reported how alkalis or  $\text{Ca}(\text{OH})_2$  released from the hydration of OPC could activate hydraulic reactions of various types of pozzolanas and mineral blended Portland cements. The current stage of knowledge upon the activation process and mechanism of slag states that when BFS enters in contact with water at higher pH (due to the presence of alkalis), Si–O, Al–O, and Mg–O bonds on the surface of glass slag break under the polarization of  $\text{OH}^-$ . This process is exothermic. Because the Ca–O and Mg–O bonds are weaker than Si–O and Al–O, a Si–Al-rich layer is formed quickly on the surface of slag grains. Then Ca ions diffuse into water solution and contribute to the precipitation of CSH, while calcium aluminosilicate hydrate can be formed on the surface of slag grain. Calorimetry has been used to detect the reactivity of different pozzolanas [16, 18]. Although the heat development from the calorimeter is able to capture different pozzolanic activities, heat is a measure of the combined Portland cement–water reaction and pozzolanic reaction in blended cement; one must understand and be able to quantify the pozzolanic

reaction. Several studies have dealt with the global effect of OPC or alkali on the activation of slag hydration and the reports on mechanical, physical properties are found in [3, 4].

This study is focused on quantitative determination of the heat evolved due to the activation effect of  $\text{Ca}(\text{OH})_2$  released from  $\text{C}_3\text{S}$  hydration and to know if this effect is proportional to the quantity of  $\text{Ca}(\text{OH})_2$ . In order to achieve the defined aim, isothermal conduction calorimetry and thermogravimetric analysis (TG)–differential thermal analysis (DTA) methods, supplemented by SEM observations and XRD method, were used.

Tricalcium silicate is one of the main crystalline phases in Portland cement with content up to 66 wt%. It exists in seven polymorphic modifications; three triclinic forms (T1, T2, and T3), three monoclinic forms (M1, M2, and M3), and one rhombohedral form (R) with similar hydraulic properties [1]. Due to the complexities of cement hydration depending on many factors,  $\text{C}_3\text{S}$  reaction with water has been used to model the hydration of cement as whole. Since almost all chemical reactions are followed by heat generation, hydration of complex system such as blended cements can be only quantified from heat evolution by using different calorimetry systems.

## Experimental

Pure  $\text{C}_3\text{S}$  phase was synthesized by means of reactions in solid state of homogenized stoichiometrical mixtures of reagent grade  $\text{CaCO}_3$  and  $\text{SiO}_2$  for  $\text{C}_3\text{S}$  at 1500 °C. Sample was burnt twice in supercanthal furnace for 2 h at corresponding temperature with intermediate grinding to a grain size of <40 µm, controlled by sieving. In both cases, the furnace was opened at burning temperature and the samples were quenched in air in order to avoid the decomposition of  $\text{C}_3\text{S}$  into  $\text{C}_2\text{S}$  and free lime. The purity of phases was controlled by XRD analysis (STOE, type theta/theta diffract meter).

BFS from Třinec, Czech Republic, was used in this experiment. The oxide composition (in mass%) is as follows:  $\text{CaO} = 38.42$ ,  $\text{SiO}_2 = 41.80$ ,  $\text{Al}_2\text{O}_3 = 6.80$ ,  $\text{Fe}_2\text{O}_3 = 0.44$ ,  $\text{K}_2\text{O} = 0.65$ ,  $\text{Na}_2\text{O} = 0.32$ ,  $\text{MgO} = 8.21$ , and  $\text{SO}_3 = 1.48$ .

The specific surface of BFS was  $425 \text{ m}^2 \text{ kg}^{-1}$  and XRD analysis showed that slag consists mainly of an amorphous phase.

Seven sample mixtures were prepared homogenizing  $\text{C}_3\text{S}$  with BFS in the proportion given in Table 1.

The isothermal calorimetry investigation was performed using an eight-channel TAM (Thermal Activity Monitor) instrument manufactured by Thermometric AB, Sweden. 6 g of dry sample powder was loaded into the glass

**Table 1** Composition (in mass%) of sample mixtures

	$\text{C}_3\text{S}$	BFS10	BFS30	BFS50	BFS70	BFS90	BFS
BFS	0	10	30	50	70	90	100
$\text{C}_3\text{S}$	100	90	70	50	30	10	0

ampoule and then hermetically closed by a plastic plug. A calculated amount of water (water-cement ratio = 0.5) is then added by using syringe and the sample is stirred inside the calorimeter in order to start the hydration process. Heat is evolved causing temperature rise. To maintain the isothermal condition, an electric power is generated to cool the calorimeter in order to keep constant room temperature. The electric power (mW) generated is proportional to the heat evolved and is continuously monitored and recorded. The time integration of power signals multiplied by a calibration coefficient gives the heat evolution and the total heat  $Q$  related to hydration process. The hydration heat is then expressed as J/g of binder (J/g gr-binder) in which gram binder (gr-binder) denotes 1 g of sample paste (mixture + water).

The data of heat flow rate were collected in a period up to 7 days and heat evolution of hydration was determined.

After a 28-day curing, the samples were crushed then ground, washed in acetone to remove free water and then air dried before they were analyzed by DTA coupled with TG instrument (DTA-Derivatograph Q-1500D) [20]. The measurements were done in alumina crucible at heating a rate of 10 °C/min in a temperature ranging from 25 to 1000 °C.

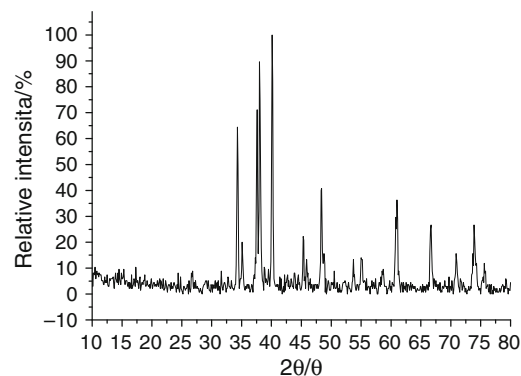
Microstructures of cement pastes after hydration and 28 days storage were studied by SEM (TESLA BS 300) to find an evidence of new hydrated products presence and their morphology.

## Results and discussion

According to the XRD pattern the synthesized product is a pure phase of  $\text{C}_3\text{S}$  with JPPCD-ICDD card No 9-0352. A very weak peak which could indicate the presence of  $\text{CaO}$  is observed at  $2\Theta = 43.840$  with  $d[\text{A}]$  value 2.396.

### Isothermal calorimetry

The courses of hydration heat evolved during 7 days of measurement by isothermal calorimetry are shown in Fig. 1. BFS has the lowest hydration heat and  $\text{C}_3\text{S}$  the highest one. If we consider that the heat evolved is proportional to the composition of mixture, then its value has to be a theoretical sum of  $H_{\text{C}_3\text{S}}$  and  $H_{\text{BFS}}$  in the proportion defined in Table 1.

**Fig. 1** XRD pattern of synthesized  $\text{C}_3\text{S}$ 

$$H_{\text{mix.}} = x_{\text{C}_3\text{S}} H_{\text{C}_3\text{S}} + x_{\text{BFS}} H_{\text{BFS}} \quad (1)$$

where  $x_{\text{BFS}}$ ,  $x_{\text{C}_3\text{S}}$ , are, respectively, BFS and  $\text{C}_3\text{S}$  contents and  $H_{\text{mix.}}$ ,  $H_{\text{BFS}}$ ,  $H_{\text{C}_3\text{S}}$  are the hydration heat of the sample mixtures, BFS and  $\text{C}_3\text{S}$ , respectively.

Then, the heat evolved due to the effect of  $\text{Ca}(\text{OH})_2$  can be estimated by the difference between calculated and measured heat of each sample mixture.

The heat  $H_{\text{ac.}}$  of the reaction between CH and BFS can be obtained from Eq. 2

$$H_{\text{ac.}} = H_{\text{exp.}} - H_{\text{mix.}} \quad (2)$$

The heat evolved during the hydration of each case depends on the amount of  $\text{C}_3\text{S}$  in the mixtures (Fig. 2). Indeed,  $\text{C}_3\text{S}$  is highly reactive in the presence of water and is responsible for the development of heat, microstructure, and other mechanical and physical properties of cement. The decrease in heat evolution depends on the content of  $\text{C}_3\text{S}$ . This dependence is not proportional because some hydration products of  $\text{C}_3\text{S}$  contribute to the hydration of BFS causing thus an additional quantity of heat.

Figure 3 shows the heat evolution of activation effect of  $\text{C}_3\text{S}$  with time. It can be seen that the activation effect depends on the amount of  $\text{C}_3\text{S}$  in mixtures, but the values are not proportional in mathematical term. Indeed, the dissolution of  $\text{C}_3\text{S}$  in water solution leads to precipitation of CSH and Portlandite– $\text{Ca}(\text{OH})_2$  that enhances the pH. Higher pH causes the partial deterioration of slag grain on the surface that liberates calcium, magnesium, and aluminum ions into solution. This process leads to the additional exothermic formation of hydrated products, as it is evidenced by calorimetry and DTA-TG analysis. Figure 2 gives an evidence of heat evolved due to the action of  $\text{Ca}(\text{OH})_2$  released from the hydration of  $\text{C}_3\text{S}$ . The curves are obtained as a function of time from Eq. 2 as difference between theoretical and experimental heat values of five sample mixtures. However, calcium hydroxide is a very stable crystallohydrates to interact with other minerals and is also submitted to other effect such as carbonation.

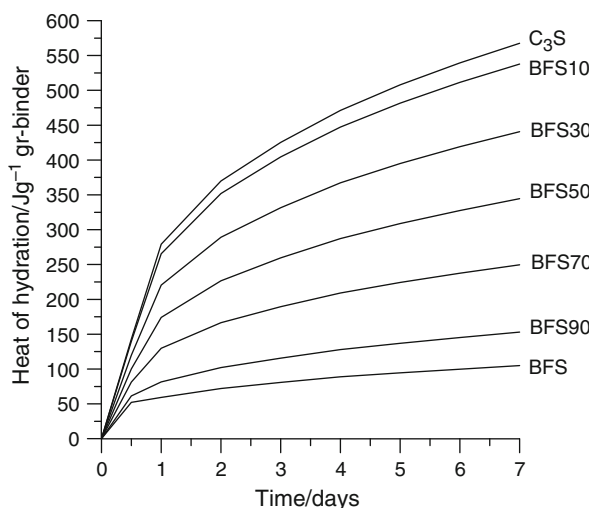


**Fig. 2** Hydration heat of samples

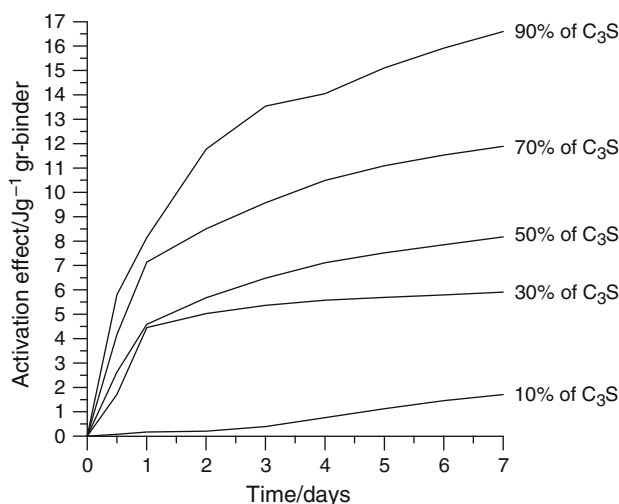


**Fig. 3** Heat of activation effect of  $\text{Ca}(\text{OH})_2$

As evidence of chemical action of  $\text{Ca}(\text{OH})_2$  upon the BFS, Table 2 reports qualitative and quantitative analysis of products formed by hydration. The table allows comparison between the amounts of hydration products in the same temperature range for different samples. DTA-TG revealed that the products formed in blended cement are calcium silicate hydrate (CSH), calcium aluminosilicate hydrate such as gehlenite hydrate ( $\text{C}_2\text{ASH}_8$ ), calcium hydroxide ( $\text{Ca}(\text{OH})_2$ ), and calcium carbonate ( $\text{CaCO}_3$ ). All  $\text{Ca}(\text{OH})_2$  are not depleted during reaction with slag. The remaining part is then partially transformed into  $\text{CaCO}_3$  by action of atmospheric air. Also, the DTA curves in some case show crystallization products such as gehlenite and akermanite.

The course of reaction can be interpreted as a function of chemically bound water after hydration. TG shows that with increasing content of  $\text{C}_3\text{S}$  in sample increases the sum of CSH, CASH, and CH amount. The presence of CSH, CH

and CC in hydrated paste characterizes the degree of  $\text{C}_3\text{S}$  hydration, but this remark is valuable for pure  $\text{C}_3\text{S}$  only, for these products could also result from the hydration of BFS. Their quantity decreases with increasing content of BFS in samples. The lower water bound in BFS attests its latent hydraulicity. The amount of calcium aluminosilicate hydrated formed increases with increasing content of  $\text{C}_3\text{S}$  in the mixture. This effect is due to the activation of CH released from  $\text{C}_3\text{S}$  hydration upon BFS. For samples with higher content of BFS, its crystallization during thermal measurement leads to the formation of gehlenite and akermanite. This exothermic process occurs in the temperatures range 850–1000 °C, in which one can observe two exothermic peaks.

#### Sample $\text{C}_3\text{S}$

The heat evolution of  $\text{C}_3\text{S}$  hydration during 7 days of monitoring can be observed in Fig. 1.

Figure 4 represents DTA-TG curves of pure  $\text{C}_3\text{S}$ . In this figure, one can observe three main temperature ranges corresponding to the decomposition of hydrated products and calcium carbonate. As free water was removed by acetone and air drying, the temperature range 25–250 °C characterized the decomposition of CSH products. Water loss from CSH decomposition ( $\text{CSH}_{\text{loss}}$ ) constitutes 6.64% in mass as determined from TG data. The second important mass loss occurred in temperatures 450–650 °C with maximal endothermic peak at 535 °C. This is attributed to the decomposition of calcium hydroxide CH ( $\text{CH}_{\text{loss}}$ ). The mass loss in this temperature range represents 8.27% in mass of total sample. The mass loss found between 650 and 850 °C is due to the decomposition of calcium carbonate formed during the air exposition. The samples were not isolated from atmosphere and an important quantity of calcium hydroxide is transformed into calcium carbonate by action of  $\text{CO}_2$ . The mass loss ( $\text{CC}_{\text{loss}}$ ) represents 4.63%.

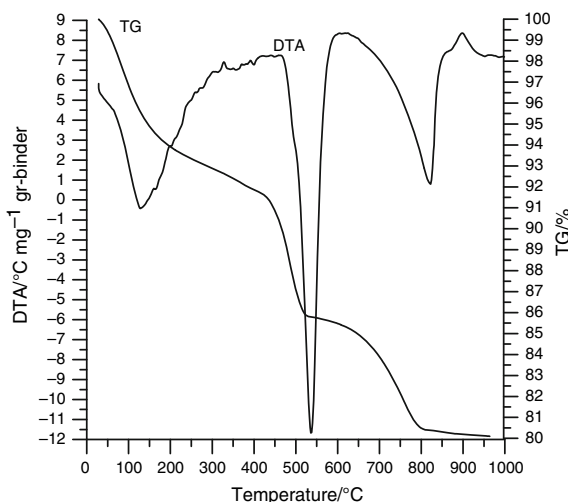
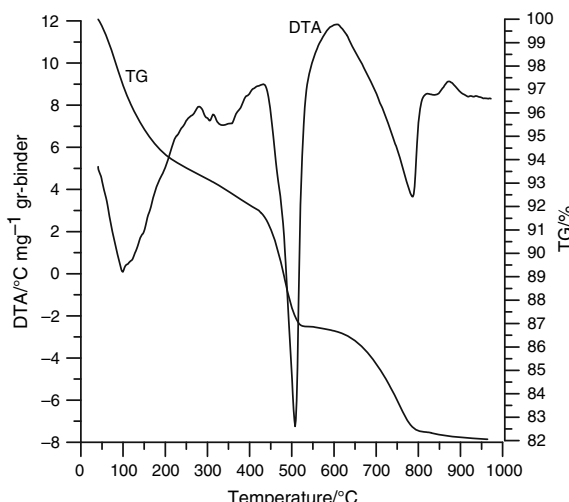
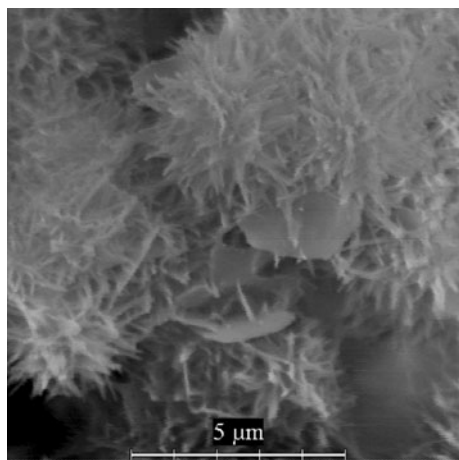
The microstructure of hydrated  $\text{C}_3\text{S}$  (Fig. 5) shows structure typical for CSH and lamellar crystals of  $\text{Ca}(\text{OH})_2$  as reported by Méducin et al. [21].

#### Sample BFS10

This sample contains 10% of BFS and 90% of  $\text{C}_3\text{S}$ . DTA-TG records indicate the characteristics similar to those of pure  $\text{C}_3\text{S}$ , but with a fundamental new endothermic peak appeared between 250 and 450 °C (Fig. 6). This peak characterizes the thermal decomposition of calcium aluminosilicate hydrates (CASH) such as gehlenite hydrate ( $\text{C}_2\text{ASH}_8$ ) formed by action of calcium hydroxide (released from  $\text{C}_3\text{S}$  hydration) upon BFS. This is the direct result of chemical reaction leading to the formation of new hydrated products. The mass loss attributed to CASH is 2.60 mass%.

**Table 2** DTA–TG characteristics and mass loss (in mass%) in different temperature intervals ( $^{\circ}\text{C}$ )

Samples	25–250/ $^{\circ}\text{C}$ CSH	250–450/ $^{\circ}\text{C}$ CASH	450–650/ $^{\circ}\text{C}$ CH	650–800/ $^{\circ}\text{C}$ CC	800–1000/ $^{\circ}\text{C}$ CP	25–1000/ $^{\circ}\text{C}$
$\text{C}_3\text{S}$	6.64		8.27	4.63	0.2	19.74
BFS10	6.35	2.60	4.66	3.98	0.19	17.78
BFS30	7.32	2.75	2.79	3.44	0.081	16.38
BFS50	7.34	3.05	2.04	2.93	0.05	15.41
BFS70	6.48	2.66	2.10	1.474	0.0737	12.78
BFS90	6.15	2.5	2.31	1.06	+0.248	12.02
BFS	4.91	1.91	0.57	0.57	+0.435	7.96

**Fig. 4** DTA–TG data measurements of  $\text{C}_3\text{S}$  paste**Fig. 6** DTA–TG data measurements of BFS10**Fig. 5** SEM micrograph of  $\text{C}_3\text{S}$  paste after 28 days

Other effect of activation is masked in thermal decomposition occurred between 25 and 250  $^{\circ}\text{C}$  by the formation of CSH, that the mass loss is 6.35%. The mass loss due to decomposition of calcium carbonate is 4.66 mass%.

Heat due to the effect of  $\text{Ca}(\text{OH})_2$  is the highest because of the amount of  $\text{C}_3\text{S}$  in mixture (Fig. 3). This difference

calculated according to Eq. 2 demonstrates that in this model the heat of reaction of CH with BFS can be identified. The additional heat results from the formation of CSH and CASH and other additional physical processes such as crystallization. The microstructure shows dominantly a CSH needle-structure (Fig. 7).

#### Sample BFS30

Calorimetric curves of heat evolution over time show a decrease in heat evolved during the hydration of BFS30, comparatively with BFS10 and  $\text{C}_3\text{S}$ . The heat due to the activation effect of CH is positive. Also this effect, in terms of hydrated products, is evident from the DTA–TG curves and microstructure.

The DTA–TG characteristics shown in Fig. 8 prove the presence of CASH (gehlenite hydrate) in temperature range 250–450  $^{\circ}\text{C}$ . Two endothermic peaks appear in this temperature range indicating the presence of other non-identified hydrated products due to the action of  $\text{C}_3\text{S}$  hydration. Also, a small endothermic peak is observed between 850 and 950  $^{\circ}\text{C}$  due to the decomposition of some carbonated product. The mass loss is negligible. For this sample BFS30  $\text{CSH}_{\text{loss}}$  is

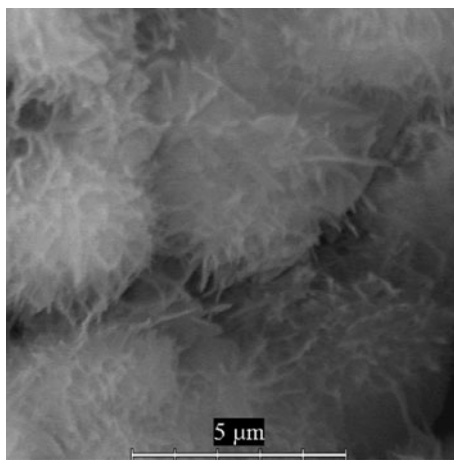


**Fig. 7** SEM micrograph of BFS10 paste after 28 days

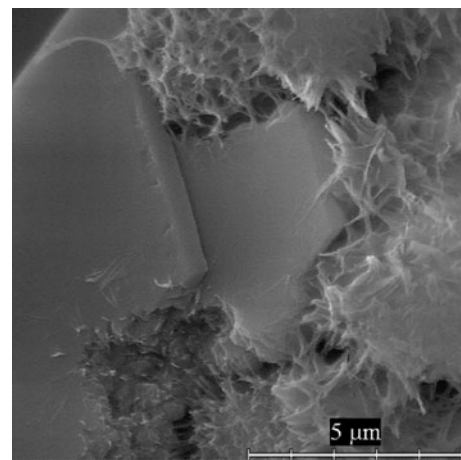


**Fig. 9** SEM micrograph of BFS30 paste after 28 days

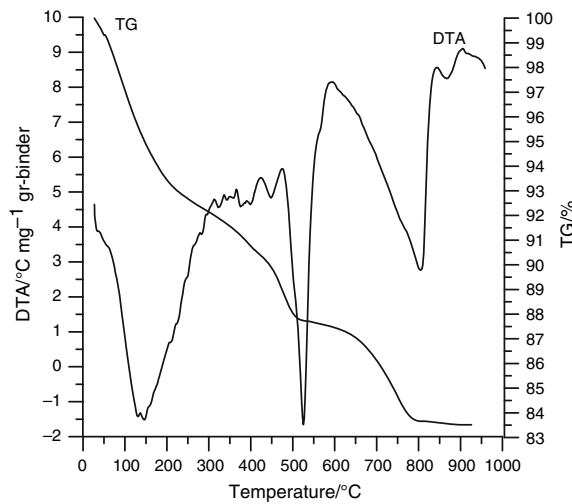


**Fig. 8** DTA–TG data measurements of BFS30

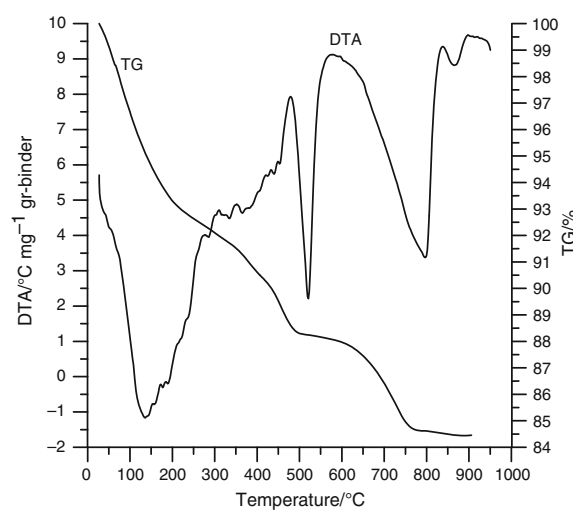


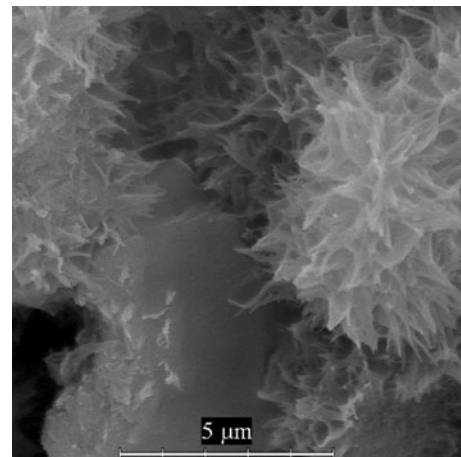
**Fig. 10** DTA–TG data measurements of BFS50

7.32%,  $\text{CASH}_{\text{loss}} = 2.75 \text{ mass\%}$ ,  $\text{CH}_{\text{loss}} = 2.79 \text{ mass\%}$ ,  $\text{CC}_{\text{loss}}$  is 3.44 mass%. The microstructure shows unhydrated deteriorating mineral grains surrounded by CSH needles (Fig. 9).

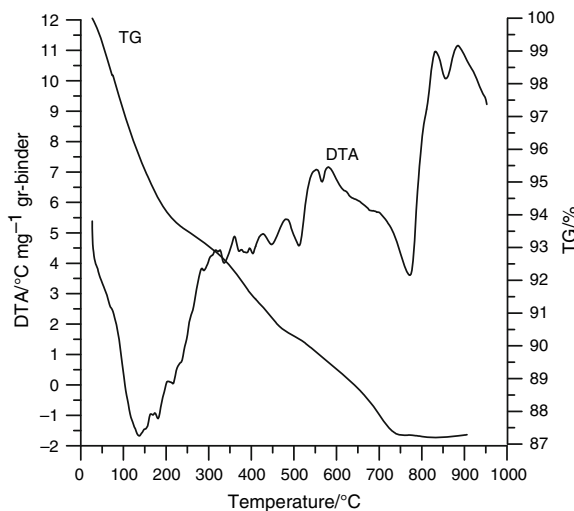
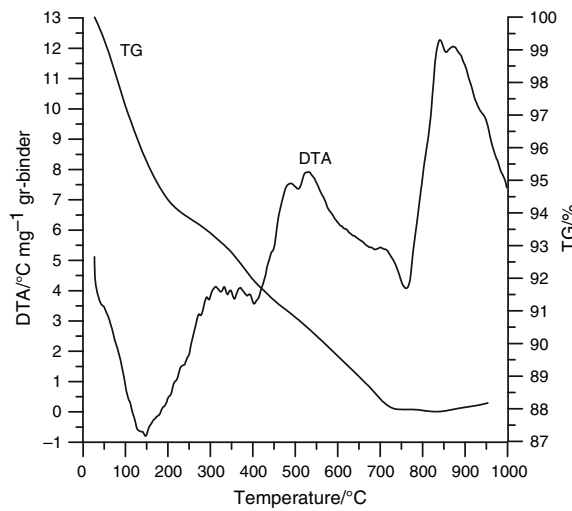
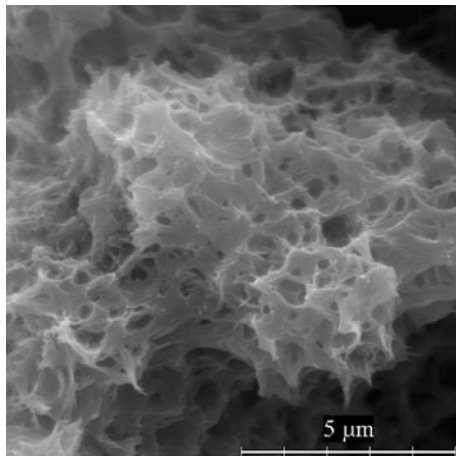
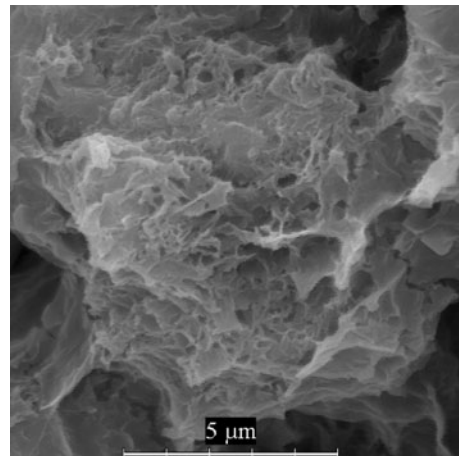
#### Sample BFS50

This sample mixture containing 50%  $\text{C}_3\text{S}$  has the same DTA–TG characteristics as the antecedent BFS30. The thermal decomposition of CSH, CASH, CH, and carbonated products is evident from Fig. 10. The total mass loss is 16.48 mass%.

The action of  $\text{Ca}(\text{OH})_2$  has decreased comparatively to the above samples.  $\text{CSH}_{\text{loss}}$  is 7.34%,  $\text{CASH}_{\text{loss}} = 3.056 \text{ mass\%}$ ,  $\text{CH}_{\text{loss}} = 2.04 \text{ mass\%}$ , and  $\text{CC}_{\text{loss}}$  is 1.47 mass%. The microstructure shown in Fig. 11 shows unhydrated mineral grains surrounded by CSH needles.



**Fig. 11** SEM micrograph of BFS50 paste after 28 days

**Fig. 12** DTA–TG data measurements of BFS70**Fig. 14** DTA–TG data measurements of BFS90**Fig. 13** SEM micrograph of BFS70 paste after 28 days**Fig. 15** SEM micrograph of BFS90 paste after 28 days

### Sample BFS70

BFS is a dominant component in the mixture BFS70. Figure 2 shows the decrease in the activation effect of  $\text{Ca}(\text{OH})_2$ , but DTA–TG show (Fig. 12) the presence of CSH, CASH, CH, and carbonated products. The total mass loss is 12.80 mass%.

$\text{CSH}_{\text{loss}}$  is 6.48%,  $\text{CASH}_{\text{loss}}$  = 2.66%,  $\text{CH}_{\text{loss}}$  = 2.10, and  $\text{CC}_{\text{loss}}$  is 1.06 mass%, respectively. Microstructure of hydrated sample is porous like (Fig. 13).

### Sample BFS90

The activation effect of CH is minimized, but positive. DTA–TG curves shown in Fig. 14 confirm the presence of CSH, CASH, CH, and CC at lower extent. It appears an exothermic peak at higher temperature due the recrystallization of glass slag during the thermal measurement.

$\text{CSH}_{\text{loss}}$  is 6.15%,  $\text{CASH}_{\text{loss}}$  = 1.96%,  $\text{CH}_{\text{loss}}$  = 0.57, and  $\text{CC}_{\text{loss}}$  is 0.57 mass%, respectively. The microstructure is porous without needle CSH (see Fig. 15).

### Sample BFS

Contrary to the well-known theory that pure BFS is hydraulically latent and could not react with water to form any hydrate products, the experimental results have proven that it has some hydration characteristics. Indeed, in water solution, fine slag grain can partially dissolve and thus release some ions, which depending on concentration can lead to the formation of new products. Also, the finesse of powder material play an important role in the surface reaction of water. Kumar et al. [22] have reported the activation of slag by simple mechanical grinding. DTA–TG curves show some endothermic and exothermic peaks in some temperature ranges (Fig. 16). The first endothermic

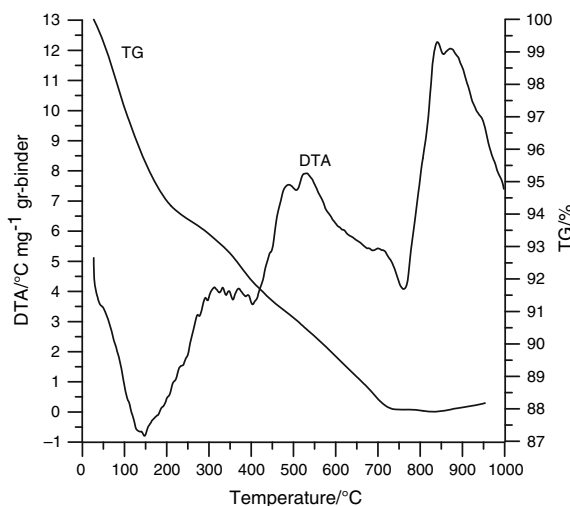


**Fig. 16** DTA–TG data measurements of BFS

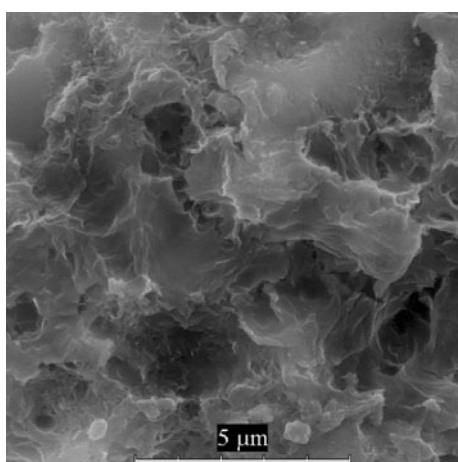


**Fig. 17** SEM micrograph of BFS paste after 28 days

peak occurs between 25 and 250 °C and like in the first six samples is related to the decomposition of CSH. The amount of the product is relatively low and represents 4.91 mass%. A little presence of CASH is detected, while CH Portlandite and carbonated products are almost absent. The most important temperature range 800–950 °C shows two exothermic peaks with maximum at 900 and 950 °C. The presence of this peak characterizes the recrystallization of glass slag into crystalline products.

To demonstrate the hydraulicity BFS, original sample without hydration has been submitted to DTA–TG measurement. The DTA curves of both samples are reported in Fig. 18. It is clear that the BFS has been hydrated. The endothermic peaks in the temperature ranges of 25–250 and 500–550 °C (although small) reveal the presence of CSH and CH products. Two endothermic peaks were found in both samples. The first one can characterize the

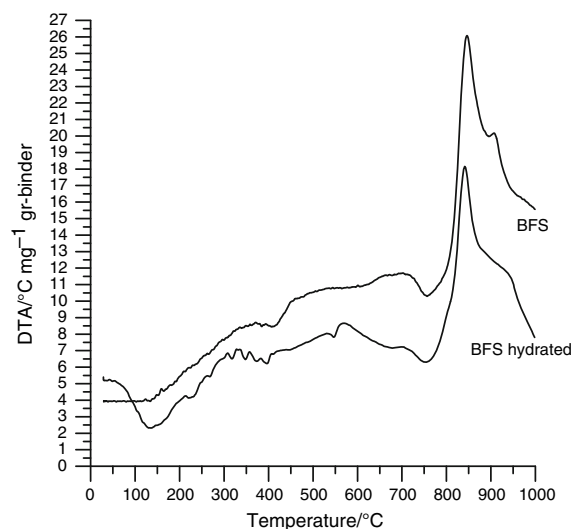


**Fig. 18** DTA of unhydrated and hydrated BFS

presence of gehlenite hydrate due to the hydration of gehlenite glass by the humidity or the presence of hydro-talcite as reported by Pérez-Ramíez and Abelló [23]. The second peak corresponds to the decomposition of calcium carbonate. The SEM in Fig. 17 shows mostly the micro-structure of unhydrated original mineral in BFS.

## Conclusions

The effect of Ca(OH)<sub>2</sub> upon the hydration of BFS can be evaluated by means of isothermal calorimetry, DTA–TG method, and SEM observation. Calcium hydroxide was released from the hydration of C<sub>3</sub>S blended with BFS and has produced, by reaction with slag grain and water, additional hydrated products. The additional heat evolved by this process can be determined by the difference between calculated theoretical heat and experimental heat, which depends on the amount of C<sub>3</sub>S in sample mixtures. The new products formed are CSH and CASH like gehlenite hydrate (C<sub>2</sub>ASH<sub>8</sub>). Generated Ca(OH)<sub>2</sub> has not been all consumed in the formation of these hydration products, but an important part remained stable or was carbonated.

**Acknowledgements** The authors wish to express their thanks to Scientific Grant Agency of the Ministry of Education of Slovak Republic and the Slovak Academy of Sciences VEGA 1/0571/08.

## References

1. Hewlett PC. Lea's chemistry of cement and concrete, 4th ed. St. Edmundsbury Press; 1998.
2. Roy DM. Alkali-activated cements, opportunities and challenges. *Cem Concr Res.* 1999;29:249–54.
3. Kourounis S, Tsivilis S, Tsakiridis PE, Papadimitriou GD, Tsibouki Z. Properties and hydration of blended cements with steelmaking slag. *Cem Concr Res.* 2007;37:815–22.

4. Xuequan W, Hong Z, Xinkai H, Husen L. Study on the steel slag and fly ash composite cement. *Cem Concr Res.* 1999;29:1103–6.
5. Ballim Y, Graham PC. Early-age heat evolution of clinker cement in relation to microstructure and composition: implications for temperature development in large concrete elements. *Cem Concr Compos.* 2004;26:417–26.
6. Doval M, Palou M, Mojumdar SC. Hydration behavior of  $\text{C}_2\text{S}$  and  $\text{C}_2\text{AS}$  nanomaterials, synthesized by sol-gel method. *J Therm Anal Calorim.* 2006;86:595–9.
7. Palou M, Majlinc J. Hydraulic activity of  $\text{C}_4\text{A}_3\overline{\text{Cr}}$  in presence of  $\text{C}_4\text{A}_3\overline{\text{S}}$ . *J Therm Anal Calorim.* 2003;71:367–73.
8. Palou MT, Majlinc J. Effects of sulfate, calcium and aluminium ions upon the hydration of sulfoaluminate belite cement. *J Therm Anal.* 1996;46:549–56.
9. Palou MT, Majlinc J. Hydration in the system  $\text{C}_4\text{A}_3\overline{\text{S}}-\text{C}\overline{\text{S}}-\text{CH}-\text{H}$ . *J Therm Anal.* 1996;46:557–63.
10. Smrčková E, Palou MT, Tomková V. Application of conduction calorimeter for study of the reactivity of  $\text{C}_2\text{S}$  in the system  $\text{C}_2\text{S}-\text{C}_4\text{A}_3\overline{\text{S}}-\text{H}$ . *J Therm Anal.* 1996;46:597–605.
11. Wadsö L, Smith ALS, Shirazi H, Mulligan SR. The isothermal heat conduction calorimeter: a versatile instrument for studying the processes in physics, chemistry and biology. *J Chem Educ.* 2001;78:1080–6.
12. Brandstetr J, Polcer J, Krátký J, Holešinský R, Havlica J. Possibilities of the use of isoperibolic calorimetry for assessing the hydration behaviors of cementitious materials. *Cem Concr Res.* 2001;31:941–7.
13. Lin F, Meyer C. Hydration kinetics modelling of Portland cement considering the effect of temperature and applied pressure. *Cem Concr Res.* 2009;39:255–65.
14. Kada-Benameur H, Wirquin E, Duthoit B. Determination of apparent activation energy of concrete by isothermal calorimetry. *Cem Concr Res.* 2000;30:301–5.
15. Huanhai Z, Xuequan W, Zhongzi X, Mingshu T. Kinetic study on alkali-activated slag. *Cem Concr Res.* 1993;23:1253–8.
16. Pane I, Hansen W. Investigation of blended cement hydration by isothermal calorimetry and thermal analysis. *Cem Concr Res.* 2005;35:1155–64.
17. Xu Q, Stark J. Early hydration of ordinary Portland cement with an alkaline shotcrete accelerator. *Adv Cem Res.* 2005;17:1–8.
18. Mertens G, Snellings R, Van Balen K, Bice-Smsir B, Vrlooy P, Elsen J. Pozzolanic reactions of common natural zeolites with lime and parameters affecting their reactivity. *Cem Concr Res.* 2009;39:233–40.
19. Codina M, Cau-dit-Coumes C, Le Bescop P, Verdier J, Ollivier JP. Design and characterisation of low-heat and low-alkalinity cements. *Cem Concr Res.* 2008;38:437–48.
20. Kuzielová E, Kovář V, Palou M. Thermal stability of  $\text{Li}_2\text{O}-\text{SiO}_2-\text{CaO}-\text{P}_2\text{O}_5-\text{F}$  glass. *J Therm Anal Calorim.* 2008;94(3):849–52.
21. Méducin F, Bresson B, Lequeux N, Noëlle de Noirfontaine M, Zanni H. Calcium silicate hydrates investigated by solid-state high resolution  $^1\text{H}$  and  $^{29}\text{Si}$  nuclear magnetic resonance. *Cem Concr Res.* 2007;37:631–8.
22. Kumar S, Kumar R, Bandopadhyay A, Alex TC, Kumar BR, Das SK, Mehrotra SP. Mechanical activation of granulated blast furnace slag and its effect on the properties and structure of Portland slag cement. *Cem Concr Res.* 2008;30:679–85.
23. Pérez-Ramírez J, Abelló S. Thermal decomposition of hydrotricalite-like compounds studied by a novel tapered element oscillating microbalance (TEOM) comparison with TG and DTA. *Thermochimica Acta.* 2006;444:75–82.